### University of Nebraska - Lincoln DigitalCommons@University of Nebraska - Lincoln

Paul Burrow Publications

Research Papers in Physics and Astronomy

8-1-2005

## Dissociative electron attachment to uracil deuterated at the N<sub>1</sub> and N<sub>3</sub> positions

A. M. Scheer University of Nebraska - Lincoln

C. Silvernail University of Nebraska - Lincoln

John A. Belot Jr. University of Nebraska - Lincoln, jbelot2@unl.edu

Gordon A. Gallup UNL, ggallup1@unl.edu

Paul Burrow pburrow1@unl.edu

Follow this and additional works at: http://digitalcommons.unl.edu/physicsburrow



Part of the Physics Commons

Scheer, A. M.; Silvernail, C.; Belot, John A. Jr.; Gallup, Gordon A.; and Burrow, Paul, "Dissociative electron attachment to uracil deuterated at the N<sub>1</sub> and N<sub>3</sub> positions" (2005). Paul Burrow Publications. Paper 33. http://digitalcommons.unl.edu/physicsburrow/33

This Article is brought to you for free and open access by the Research Papers in Physics and Astronomy at Digital Commons@University of Nebraska -Lincoln. It has been accepted for inclusion in Paul Burrow Publications by an authorized administrator of Digital Commons@University of Nebraska -Lincoln.

Submitted April 12, 2005; revised May 27, 2005; published online June 22, 2005.

# Dissociative electron attachment to uracil deuterated at the $N_1$ and $N_3$ positions

A.M. Scheer a, C. Silvernail b, J.A. Belot b, K. Aflatooni a, l, G.A. Gallup a, and P.D. Burrow a,\*

**Abstract:** Deuteration at the nitrogen sites of uracil produces a striking change in the dissociative attachment cross-section at electron energies below 3 eV. In particular, sharp structures observed in uracil are absent or too small to observe. This result, as well as theoretical modeling, supports the earlier assignment of the sharp structure to vibrational Feshbach resonances that decay by tunneling of the  $N_1$  hydrogen atom through the barrier created by the avoided crossing of the dipole bound anion potential surface by that of the lowest  $^2\Sigma$  valence anion state.

#### 1. Introduction

In an earlier work [1], sharp structure appearing in the dissociative electron attachment (DEA) cross-section of uracil [2] and the halo-uracils [3] at energies below 4 eV was attributed in part to vibrational Feshbach resonances (VFRs) [4] associated with the dipole bound anion state (DBS) of uracil. In brief, it was argued that mixing of this diffuse electronic state with the lowest lying valence anion state of  ${}^{2}\Sigma$  symmetry predissociates the dipole bound state, allowing those vibrational levels lying above the threshold energy for the DEA process to contribute to bond breaking. In the case of uracil, calculations indicate that the molecular orbital in which an electron attaches to form the lowest  ${}^{2}\Sigma$  valence anion state is strongly antibonding between N<sub>1</sub> and H. Consequently, temporary occupation of this orbital excites N<sub>1</sub>-H stretching vibrations in preference to other possible modes.

Combining the dipole binding energy of ≈90 meV

as determined by photoelectron spectroscopy [5] and [6] and the  $N_1$ -H stretch vibrations of the neutral molecule (0.432 eV) [7], the sharp structures appearing at 0.69 and 1.01 eV in the production of  $(U-H)^-$ , the parent anion minus a H atom, [2] were identified with electron attachment to and decay of the v=2 and 3 vibrational levels of the DBS. The v=1 level lies below the DEA threshold and cannot contribute. However, this latter VFR is observed in the halo-uracils not only in DEA [3] but in the total electron scattering cross-section [1].

Proof that the sharp structure in the DEA cross-section arises from ejection of a hydrogen atom residing on a nitrogen rather than on a carbon atom was provided by Abdoul-Carime et al. [8] in thymine, which is identical to uracil except for a methyl group rather than a hydrogen atom bound to  $C_5$ . Using thymine deuterated only on the carbon positions,  $T_d$ , mass analysis showed that only  $(T_d-H)^-$  appeared below electron energies of 4 eV, and that there was no contribution from  $(T_d-D)^-$ . Furthermore, the yield characteristics were essentially iden-

<sup>&</sup>lt;sup>a</sup> Department of Physics and Astronomy, University of Nebraska-Lincoln, Lincoln, NE 68588-0111, United States

<sup>&</sup>lt;sup>b</sup> Department of Chemistry, University of Nebraska-Lincoln, Lincoln, NE 68588-0111, United States

<sup>&</sup>lt;sup>1</sup> Permanent address: Department of Physics, Fort Hays State University, Hays, KS 67601-4099, United States.

<sup>\*</sup> Corresponding author. Email: pburrow1@unl.edu

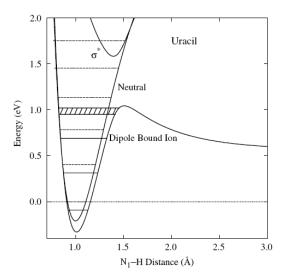


Fig. 1. Potential energy curves for uracil along the  $N_1$ –H stretching coordinate. The vibrational levels of the neutral molecule are shown as dashed lines, those for the dipole bound anion as solid lines.

tical to that of undeuterated thymine.

Calculated potential curves for the dipole bound and valence anion states and the neutral molecule as a function of the N<sub>1</sub>-H stretch coordinate are shown in Fig. 1. The methods used to obtain these are described later. The energies and widths of the sharp structures in the DEA cross-section suggest that H tunneling through the barrier created by the avoided crossing between the dipole and valence anion states is a key feature of the DEA process. Indeed, in the high-energy resolution measurements of Denifl et al. [2], the peak at 1.01 eV, near the top of the barrier, is much broader than that at 0.69 eV, which is narrow and may still be instrumentally unresolved. These considerations indicate that deuteration at the nitrogen atom sites should cause significant changes in the shape of the DEA cross-section below 4 eV, owing to differences in tunneling probability as well as shifts in the energies of the vibrational levels producing the peaks. In this Letter, we confirm this experimentally and provide theoretical support for this interpretation as well.

#### 2. Experimental results

In this study, we observe the total yield of negative ions in an electron transmission apparatus, modified to collect ion current inside the collision cell. The advantage of this instrument is that the collision cell and an attached sample oven may be separately heated to produce the required target density. In the transmission mode, it

was used previously to locate the temporary negative ion states of the DNA bases [9]. Because of the relatively short cell length, its geometry is not optimum for DEA measurements, and end effects may cause differences in collection efficiency for thermal ions and more energetic fragments. Efforts were made to keep the collision cell as electric field-free as possible.

Uracil, deuterated at the N<sub>1</sub> and N<sub>3</sub> positions, was produced by standard methods [10]. The <sup>1</sup>H NMR spectrum indicated that the purity of the sample was  $92 \pm 5\%$ . Fig. 2 shows the total yield of negative ion fragments as a function of electron energy in uracil (upper curve) and 1,3-deuterated uracil (lower curve). Except for the poorer electron energy resolution, the shape of the anion yield below 3 eV in uracil is consistent with the work by others [2], and the energy scale has been calibrated using the strong peak reported at 1.01 eV. This peak and the small, unresolved peak at 0.69 eV are the principal features assigned earlier [1] to VFRs. The broader feature at 1.7 eV is coincident with the energy of the second  ${}^{2}\Pi$  anion state of uracil as observed [9] using electron transmission spectroscopy. Coupling between such  $\Pi$  and repulsive  $\Sigma$  states induced by out-of-plane motions is well known to contribute to the DEA process in planar unsaturated hydrocarbons. Above 4 eV, contribu-

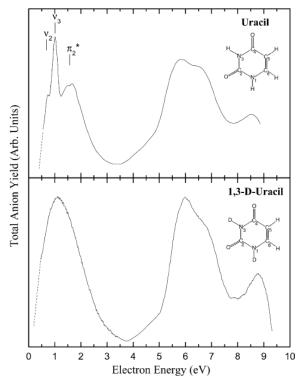


Fig. 2. The total anion current as a function of electron energy in uracil (upper panel) and 1,3-deuterated uracil (lower panel). Above ~8.5 eV, the onset of positive ion current overwhelms the anion production.

tions to DEA from core-excited anion states are present and the mass analyzed spectra of Denifl et al. [2] show that fragment anions of a number of different masses are produced. Above ~8.5 eV, the anion current is diminished and ultimately obscured by the onset of positive ionization [11].

In striking contrast to uracil, the deuterated compound at low energies shows no evidence of sharp VFRs, confirming our expectation that isotopic changes at the  $N_1$  site should greatly influence the DEA spectrum. The broad peak we observe has its maximum at 1.16 eV, as calibrated by admission of  $N_2O$  and reference to the DEA peak of the latter compound at 2.25 eV.

We expect the differences in the yields to arise primarily from two effects. First, the vibrational levels associated with the N<sub>1</sub>-D stretch, 0.322 eV [10], are reduced relative to those of N<sub>1</sub>-H, 0.432 eV. Thus, the positions of the VFRs relative to the barrier indicated schematically in Fig. 1 are different. The energies of the vibrational levels near the top of the barrier are, of course, anharmonic. This can be gauged in uracil by comparing the expected location of v = 3 if the levels were harmonic, 1.21 eV, with that of the measured 1.01 eV peak. Fortuitously, in deuterated uracil, v = 4 would lie at 1.20 eV if harmonic, and thus we could expect this VFR to lie rather close to that for v = 3 in uracil. This assumes, of course, that the dipole binding energy is the same as that of uracil. The absence of a sharp feature in our data could therefore be a consequence, in part, of the reduced tunneling rate of a deuterium atom through the barrier because of its greater mass. Such a VFR could be substantially narrower in width and, thus, not observable with our energy resolution.

#### 3. Theoretical results

To test the credibility of this conjecture, we have made preliminary calculations of the size of the interaction between the two important diabatic states, namely the DBS and the lowest valence  $^2\Sigma$  anion state. In all of these calculations a 6-31G(d) basis set was used for the valence orbitals. The DBS orbital was represented by four Gaussian sets of {s, p<sub>x</sub>, p<sub>y</sub>, p<sub>z</sub>} with scale factors of 0.04, 0.004, 0.0004, and 0.00004. For convenience, we symbolize the DBS orbital as  $\sigma_{\text{DBS}}$  and the N<sub>1</sub>–H antibonding orbital as  $\sigma^*$ . Briefly, the procedure was as follows:

1. We construct two N + 1-electron  ${}^{2}\Sigma$  functions with a uracil core (symbolized by C),

$$\Psi_{\rm D} = [\mathbf{C}\sigma_{\rm DBS}],\tag{1}$$

$$\Psi_{\sigma}^{*} = [\mathbf{C}'\sigma^{*}], \tag{2}$$

where each of these was determined with a conventional ROHF procedure. The only difference is that  $\Psi_{\rm D}$  is determined with the whole basis set, whereas  $\Psi_{\sigma}^{*}$  does not include the 16 diffuse dipole AOs. The cores are therefore somewhat different and we note this with the prime symbol ' in Eq. (2). Although this requires the later use of a nonorthogonal CI, it conveniently provides each function as the ground state of its configuration in the ROHF. The two-state CI calculations for different N<sub>1</sub>-H distances yield two potential curves with an avoided crossing in which the minimum gap is 0.602 eV at an extension of 0.350 beyond the equilibrium length. During this procedure, the relative positions of all the other atoms were held fixed with respect to one another<sup>2</sup>. We note that Sommerfeld [12] has studied the interaction between the DBS and the  ${}^{2}\Pi(\pi_{1}^{*})$  resonance in uracil for puckered ring geometries, finding a much smaller coupling.

- 2. The interaction energy is critical only at the avoided crossing point and was used with various empirical quantities to construct the Morse function based curves shown in Fig. 1. The diabatic  $\sigma^*$  potential curve was modeled with an asymptotic energy of 0.6 eV and a vertical attachment energy (VAE) of 2.5 eV. The latter and the slope of the curve at the VAE were varied to obtain the best agreement with the experimental VFR peaks.
- 3. We now use the lower of the two adiabatic curves we have calculated,  $\psi_{\text{adiabat.}}(r,R)$ , where r and R stand for the electronic and nuclear coordinates, respectively, to estimate the DEA signals due to the VFRs. If the original upper diabatic valence state were not present, the dipole state and the neutral-plus-continuum-electron state,  $\psi_{s}$ , would be very close to parallel, and there would be essentially no coupling. Any effects due to VFRs would be exceedingly weak. In the presence of the upper state, however, considerable vibronic coupling between electronic wave functions is expected from the  $\mathrm{á}\psi_{\varepsilon}(r,\!R)|\partial/\partial R|\psi_{\mathrm{adiabat.}}(r,\!R)$ ñ and  $άψ_ε(r,R)|∂^2/∂R^2|ψ_{adiabat}(r,R)$ ñ terms in the electronic matrix element. Thus, very approximately, we expect the DEA due to VFRs to be proportional to the energy dependent Franck-Condon factors (FCF) between the initial and final vibrational states times an average over the vibronic coupling terms. If the average is sufficiently independent of the vibrational state, the relative DEA peaks should just be proportional to the FCFs. Sommerfeld has given much the same argument [13].

Fig. 3 illustrates the computed FCFs on a log scale as a function of the electron impact energy for both uracil and 1,3-deuterated uracil. Rather good agreement is found in the energies of the uracil VFRs with respect to those measured experimentally. The natu-

<sup>&</sup>lt;sup>2</sup> The calculations were performed with locally constructed programs described in http://phy-ggallup.unl.edu/crunch/.

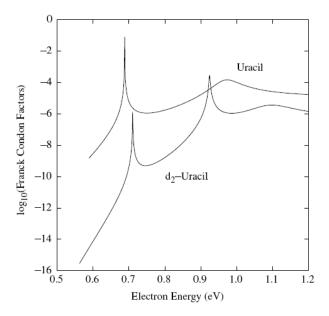


Fig. 3. Semi-log plot of the calculated Franck-Condon factors (FCF) as a function of electron energy for uracil and 1,3-deuterated uracil.

ral widths of the two features are substantially different, the lower peak possessing a calculated full-width at half-height (FWHH) of 5.73 µeV and the upper with a value of 0.04 eV, reflecting the differences in the barrier at the two energies through which the hydrogen atom must tunnel. In Fig. 4, the FCFs of Fig. 3 are convoluted with an electron energy distribution of 80 meV (FWHH) and shown as a function of electron energy.

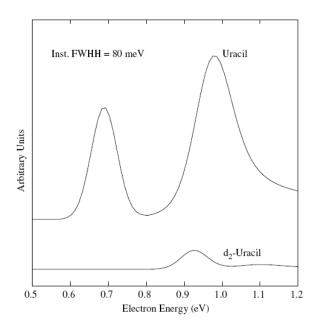


Fig. 4. Calculated Franck-Condon factors, convoluted with an electron distribution of 80 meV FWHH, as a function of electron energy.

When compared with experiment, the differences in relative heights and widths suggest that the calculated widths are too narrow. This may reflect the 'diatomic' approximation used in our calculations, when in fact the  $N_1$ -H stretch is accompanied by other vibrational modes as well, driven by occupation of the lowest  $\sigma^*$  valence orbital. Nevertheless, the calculations indicate that the VFRs in the deuterated compound will appear much smaller than in uracil. The calculated natural width of the VFR between 0.9 and 1.0 eV is 2.8 meV, suggesting that this feature might be observed in the deuterated compound if higher energy resolution were employed.

The broad feature appearing at 1.16 eV in 1,3-deuterated uracil, see Fig. 2, lies  $\approx$ 0.5 eV below the second  $^2\Pi$  anion state at 1.7 eV. A portion of the anion yield may arise from the  $^2\Pi_2/^2\Sigma$  coupling mechanism invoked to explain the peak in uracil near 1.7 eV. In this case, the higher thermal populations of the N–D modes relative to those of N–H in uracil might account for increased coupling and a shift to lower energy. A contribution from one or more broad VFRs near the top of the barrier cannot be ruled out.

Finally, we note that the treatment given here is quite approximate and deals only with the one  $N_1$ –H stretching mode. Examination of the lowest valence  $\sigma^*$  orbital of uracil indicates that other vibrational modes are also excited but may be too narrow to appear in the published yields. Attention should be called to electron occupation of the upper adiabatic state as well. The lower vibrational levels of this state, calculated to be spaced by  $\approx 300$  meV, may also contribute to DEA yields, causing broader structures appearing above 1 eV.

#### Acknowledgments

Thanks to Ilya Fabrikant for useful discussions on VFRs. C.S. and J.A.B. were supported by the Nebraska Research Initiative.

#### References

- [1] A.M. Scheer, K. Aflatooni, G.A. Gallup and P.D. Burrow, *Phys. Rev. Lett.* **92** (2004), p. 068102.
- [2] S. Denifl, S. Ptasinska, G. Hanel, B. Gstir, M. Probst, P. Scheier and T.D. Märk, *J. Chem. Phys.* **120** (2004), p. 6557 (references therein).
- [3] S. Denifl, S. Matejcik, B. Gstir, G. Hanel, M. Probst, P. Scheier and T.D. Märk, J. Chem. Phys. 118 (2003), p. 4107
- [4] H. Hotop, M.-W. Ruf, M. Allan and I.I. Fabrikant, *Adv. Atom. Mol. Opt. Phys.* **49** (2003), p. 85.
- [5] J.H. Hendricks, S.A. Lyapustina, H.L. de Clercq, J.T.

- Snodgrass and K.H. Bowen, *J. Chem. Phys.* **104** (1996), p. 7788.
- [6] J. Scheidt, R. Weinkauf, D.M. Neumark and E.W. Schlag, *Chem. Phys.* **239** (1998), p. 511.
- [7] P. Colarusso, K. Zhang, B. Guo and P.F. Bernath, *Chem. Phys. Lett.* **269** (1997), p. 39.
- [8] H. Abdoul-Carime, S. Gohlke and E. Illenberger, *Phys. Rev. Lett.* **92** (2004), p. 168103.
- [9] K. Aflatooni, G.A. Gallup and P.D. Burrow, J. Phys. Chem. A 102 (1998), p. 6205.
- [10] A.J. Barnes, M.A. Stuckey and L. Le Gall, *Spectrochim. Acta* 40A (1984), p. 419.
- [11] K. Aflatooni, A.M. Scheer and P.D. Burrow, *Chem. Phys. Lett.* **408** (2005), p. 426.
- [12] T. Sommerfeld, J. Phys. Chem. A 108 (2004), p. 9150.
- [13] T. Sommerfeld, J. Phys. Conf. Ser. 4 (2005), p. 245.